

New Angular-Shaped and Isomerically Pure Anthradithiophene with Lateral Aliphatic Side Chains for Conjugated Polymers: Synthesis, Characterization, and Implications for Solution-Processed Organic Field-Effect Transistors and Photovoltaics

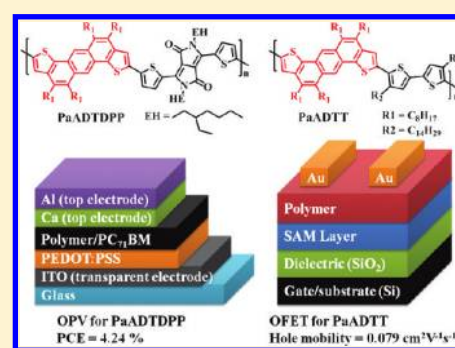
Jhong-Sian Wu, Chung-Te Lin, Chien-Lung Wang, Yen-Ju Cheng,* and Chain-Shu Hsu*

Department of Applied Chemistry, National Chiao Tung University, 1001 Ta Hsueh Road, Hsin-Chu, 30010 Taiwan

Supporting Information

ABSTRACT: An isomerically pure anti-anthradithiophene (aADT) arranged in an angular shape is developed. Formation of the framework of aADT incorporating four lateral alkyl substituents was accomplished by a one-pot benzannulation via multiple Suzuki coupling. This newly designed 2,8-stannylated aADT monomer was copolymerized with a dithienodiketopyrrolopyrrole (DPP) unit and a bithiophene unit, respectively, to furnish an alternating donor–acceptor copolymer poly(anthradithiophene-*alt*-dithienodiketopyrrolopyrrole) (PaADTDPP) and a thiophene-rich poly(anthradithiophene-*alt*-bithiophene) (PaADTT). PaADTT with crystalline nature achieved a high FET mobility of $7.9 \times 10^{-2} \text{ cm}^2 \text{ V}^{-1} \text{ s}^{-1}$ with an on–off ratio of 1.1×10^7 . The photovoltaic device based on the PaADTDPP:PC₇₁BM (1:2.5, w/w) blend exhibited a V_{oc} of 0.66 V, a J_{sc} of 9.49 mA/cm², and a FF of 58.4%, delivering a power conversion efficiency (PCE) of 3.66%. By adding 1.5 vol % 1-chloronaphthalene (CN) as a processing additive, the PCE can be improved to 4.24%. We demonstrated that these angular-shaped and alkylated aADT-based polymers have better organic photovoltaic (OPVs) and field-effect transistor (FETs) characteristics than the linear-shaped ADT-containing polymers.

KEYWORDS: anthradithiophene, benzannulation, solar cells, field-effect transistors



INTRODUCTION

Solution-processed organic photovoltaics (OPVs) and organic field-effect transistors (OFETs) have received tremendous scientific and industrial interest in recent years due to their cost-effective and mechanically flexible advantages.¹ Development of advanced p-type conjugated polymers continues to play a pivotal role to drive high efficiency of OPVs and high mobility of OFETs. Considerable effort has been devoted to designing and synthesizing multifused aromatic small molecules, which can ultimately be used to construct solution-processable conjugated polymers.² The acenedithiophene family, where polyaromatic benzene rings are fused with two terminal thiophene rings, are particularly attractive and promising building blocks.³ First, α -positions of the two end-capped thiophenes can be selectively functionalized for easy and precise cross-coupling polymerization. Second, integration of thiophene and benzene rings into a rigid and coplanar entity facilitates π -electron delocalization and induces strong π - π stacking for efficient charge transporting.⁴ Third, the aromatic size and molecular shape of the acenedithiophene system are chemically manipulable to tailor the electronic and steric properties.^{3a,4a,c} Incorporation of the shortest acenedithiophenes, that is, benzodithiophene (BDT), into a variety of conjugated polymers has produced highly efficient organic field-effect transistors (OFETs) and bulk heterojunction (BHJ) polymer solar cells (PSCs).^{3b,5} Pentacene is the most

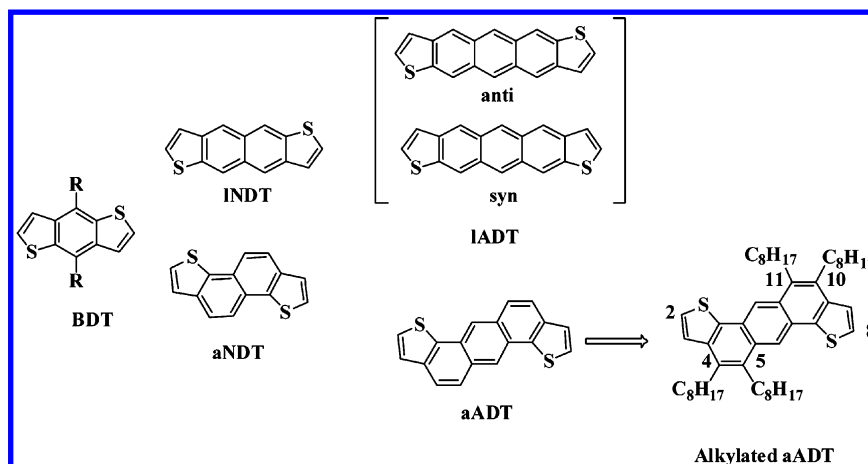
representative semiconductor to realize the highest mobility of OFETs but is also known for being poorly stable against photoinduced oxidation.⁶ Linear-fused anthradithiophene (IADT) derivatives not only exhibit comparable OFET mobilities to pentacene but also possess many advantages, including easier functionalization, broader absorption window, and better chemical stability.^{4d,e,7} Nevertheless, the polymers incorporating IADT units are only sporadically reported.⁸ One problem at the molecular level is that introducing two alkyl chains on the 5, 10 positions of IADT units is not sufficient to warrant solubility of the resulting polymers for solution-processing. Furthermore, the traditional synthesis of the linear-fused ADT inevitably afforded an inseparable mixture of syn- and anti-isomers resulting in undefined molecular conformation.^{7c,9} So far the PSC devices using the IADT-based polymers have only shown power conversion efficiencies (PCE) less than 1%.⁸ Recently, Takimiya and co-workers demonstrated that the shape of the naphthodithiophene (NDT) motif plays a critical role in polymer packing (Scheme 1).¹⁰ In contrast to the polymer with the linear-fused NDT units, the copolymer incorporating the angular-fused NDT units can pack into highly ordered structures, thereby achieving higher FET mobilities.

Received: April 17, 2012

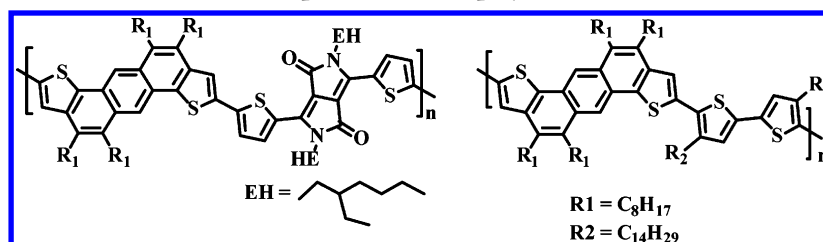
Revised: May 18, 2012

Published: May 23, 2012

Scheme 1. Chemical Structures of Acenedithiophene Derivatives, BDT, INDT, aNDT, IADT, aADT, and Laterally Alkylated aADT



Scheme 2. Chemical Structures of the Anthradithiophene-Based Copolymers, PaADTDPP and PaADTT



It was also reported that angular-fused ADT (aADT) has a lower-lying HOMO energy level than IADT, which could be beneficial for better air stability and greater open-circuit voltage (V_{oc}) for PSCs.^{3a} On the basis of the aforementioned considerations, it is promising and desirable to develop an angular-fused ADT for preparing a new class of ADT-based polymers for FET as well as OPV applications (Scheme 1). Despite the fact that the synthesis of the angular-shaped aADT small molecule has been reported previously,¹¹ the absence of aliphatic side chains as solubilizing groups restricted its practical application for polymer synthesis. To circumvent this deficiency, we present here a useful and facile synthesis to prepare an isomer-free aADT with the implantation of four lateral alkyl substituents at its 4, 5 and 10, 11 positions (Scheme 1). The synthesis of aADT is simply accomplished by one-pot benzannulation via multiple Suzuki coupling. This newly designed 2,8-stannylated aADT monomer was copolymerized with a dithienodiketopyrrolopyrrole (DPP) unit and a bithiophene unit, respectively, to furnish an alternating donor–acceptor copolymer poly(anthradithiophene-*alt*-dithienyl-diketopyrrolopyrrole) (PaADTDPP) and a thiophene-rich poly(anthradithiophene-*alt*-bithiophene) (PaADTT) (Scheme 2). The synthesis, characterization, and applications of these polymers in PSCs and FETs will be discussed.

RESULTS AND DISCUSSION

Synthesis of Monomers and Polymers. The synthesis of the monomers Sn-aADT is depicted in the Scheme 3. Lithiation of 1-decyne (1) was followed by reacting with 1-bromooctane yielded 9-octadecyne (2). Pt-catalyzed *syn*-diborylation of bis(pinacolato)diboron with 2 afforded dioctyl-bis-(pinacolatoboryl)alkene (3) in 75% yield.¹² The 2,2'-(2,5-dibromo-1,4-phenylene)bis(3-bromothiophene) (7) was prepared

by Negishi coupling of (3-bromothiophen-2-yl)zinc(II)-bromide (5) with 1,4-dibromo-2,5-diiodobenzene (6).¹³ In the presence of $\text{Pd}(\text{PPh}_3)_4$ as the catalyst, aADT was successfully synthesized by tandem Suzuki-Miyaura cross-coupling of 7 with diborylalkene (3) in good reaction yield of 59%.¹⁴ This strategy is very efficient and useful in view of forming the aADT framework with concomitantly introducing four flanking octyl chains. It is also the first example that double benzannulation by Suzuki coupling can be carried out through a benzene-thiophene-type dibromobiaryl substrate. Note that the length of alkyl chains can be easily adjustable depending on preparation of the dialkyldiborylalkene analogues. Lithiation of aADT by *t*-butyllithium to react with trimethyltin chloride resulted in the formation of Sn-aADT in almost quantitative yield (99%). Monomer Sn-aADT was copolymerized with 3,6-bis(5-bromothiophen-2-yl)-2,5-bis(2-ethylhexyl)pyrrolo[3,4-*c*]pyrrole-1,4(2*H*,5*H*)-dione (8) and 5,5'-dibromo-4,4'-ditetradecyl-2,2'-bithiophene (9) by Stille coupling to give PaADTDPP and PaADTT, respectively (Scheme 3). The molecular weights of PaADTDPP and PaADTT are not obtainable due to their low solubilities in tetrahydrofuran at room temperature.

Thermal Properties. The thermal stability was analyzed by thermogravimetric analysis (TGA). PaADTDPP and PaADTT exhibited sufficiently high decomposition temperatures (T_d) of 400 and 434 °C, respectively, indicating that PaADTT is thermally more stable than PaADTDPP (Figure S1 in Supporting Information). On the basis of the differential scanning calorimetry (DSC) analysis, PaADTDPP is amorphous, while bithiophene-based PaADTT showed crystalline nature with the observation of the melting point at 285 °C during heating and the crystallization point at 276 °C upon cooling (Figure 1).

Scheme 3. Synthetic Route for the Angular-Fused Anthradithiophene Unit and the Corresponding Copolymers

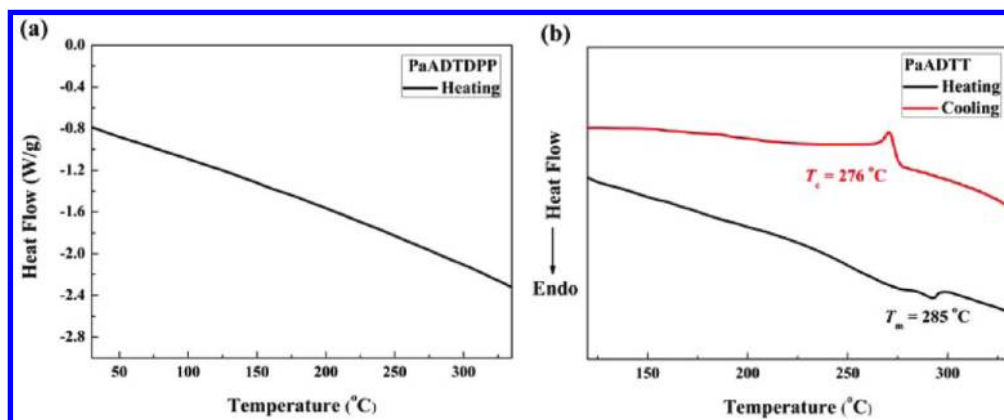
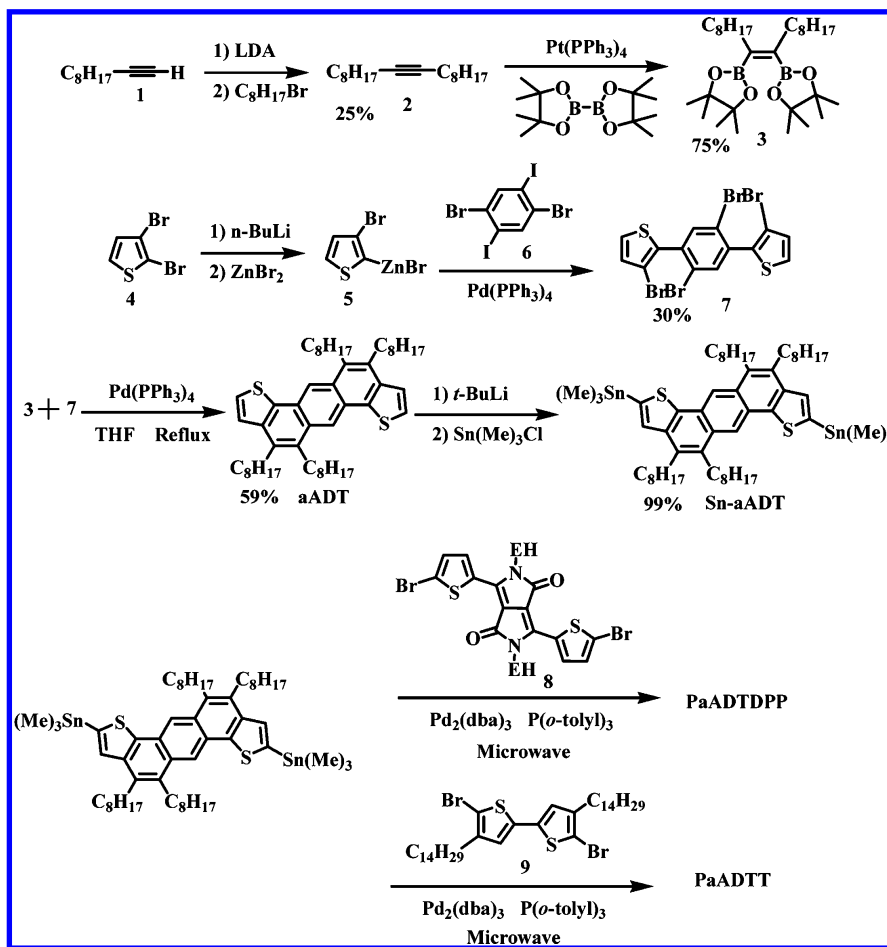


Figure 1. Differential scanning calorimetry of PaADTDPP (a) and PaADTT (b).

Optical Absorption. The absorption spectra of the monomer and polymers are shown in Figure 2. The absorption spectrum of the aADT monomer consists of three sharp peaks with narrow bandwidth (Figure 2a). Besides, small bands at lower energy of 362, 383, and 403 nm, which are presumably attributed to vibronic transitions, in toluene solution were also observed. These characteristics clearly reflect the highly rigid and coplanar feature of the anthradithiophene unit. For PaADTDPP, the shorter wavelength absorbance comes from the $\pi-\pi^*$ transition of the pentacyclic units, while the lower energy band is ascribed to the intramolecular charge transfer (ICT) between the electron-rich and the electron-deficient

DPP unit (Figure 2b). The donor–acceptor PaADTDPP copolymer showed a narrow optical band gap (1.39 eV) deduced from the absorption edge of solid state spectra. Besides, PaADTDPP showed a tailing of the absorption band with a shoulder around 850 nm in the solid state. The origin of this shoulder presumably comes from strong intermolecular interactions. The absorption spectra of PaADTDPP in the solution and solid states are essentially unchanged, whereas PaADTT showed significant red-shifted absorption in the solid state due to the stronger $\pi-\pi$ stacking and higher degree of the intermolecular ordering (Figure 2c). Also note that a new shoulder peak at 553 nm is developed in the solid state. These

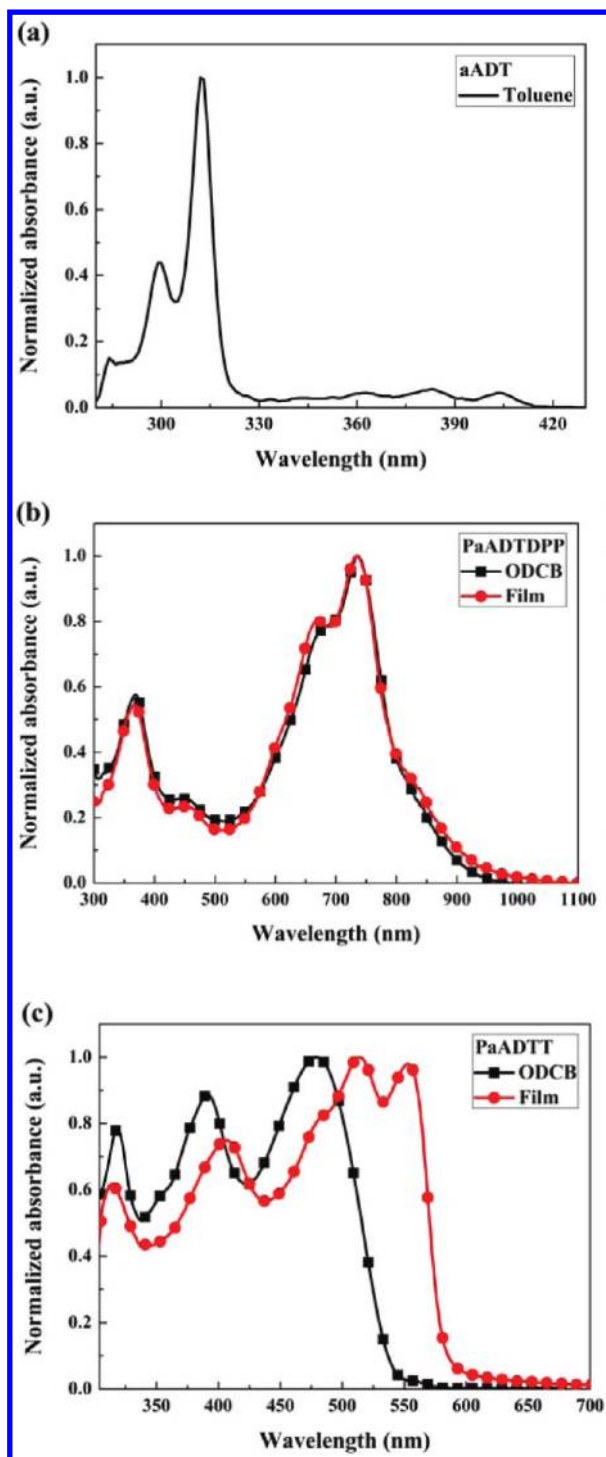


Figure 2. Normalized absorption spectra of aADT in toluene solution (a), PaADTDPP (b), and PaADTT (c) in *o*-dichlorobenzene (ODCB) solution and the solid state.

phenomena are rather consistent with the crystalline nature of PaADTT.

Electrochemical Properties. Cyclic voltammetry (CV) was employed to examine the electrochemical properties and evaluate the highest occupied molecular orbital (HOMO) and lowest unoccupied molecular orbital (LUMO) levels of the polymers (Table 1 and Figure 3). The two polymers showed

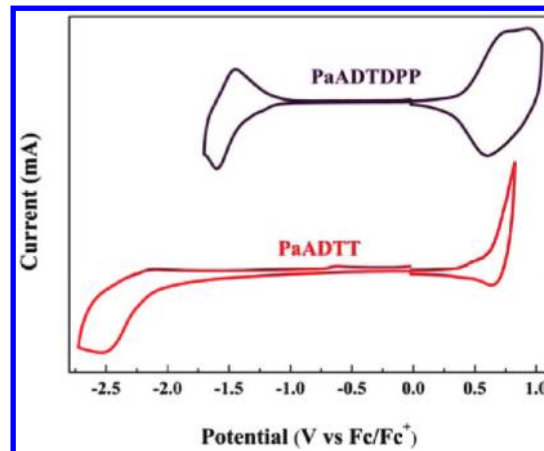


Figure 3. Cyclic voltammograms of PaADTDPP and PaADTT in the thin film at a scan rate of 50 mV/s.

stable and reversible p-doping/n-doping process in the cathodic and anodic scans. The HOMO levels being estimated to be -5.21 eV for PaADTDPP and -5.41 eV for PaADTT are at ideal range to ensure better air stability and greater attainable V_{oc} in the final device. The LUMO level is located at -3.61 eV for PaADTDPP, which is positioned 0.2 eV above the LUMO level of the PC₇₁BM (-3.8 eV) to induce energetically favorable electron transfer. However, the LUMO energy level of PaADTT is -3.0 eV, which might be too high relative to the LUMO level of PC₇₁BM.

Characteristics of Organic Field-Effect Transistors. To evaluate the FET hole mobilities of the aADT-based polymers, the devices using a bottom-gate, top-contact configuration with evaporated gold source/drain electrodes (40 nm in thickness) were fabricated. The output and transfer plots of the devices exhibited typical p-channel OFET characteristics (Figure 4). The hole mobilities were deduced from the transfer characteristics of the devices in the saturation regime. The PaADTDPP-based OFETs using unmodified SiO₂ as gate dielectric produced the hole mobilities of 2.0×10^{-3} and 9.4×10^{-3} cm² V⁻¹ s⁻¹ with the annealing temperature at 150 and 250 °C, respectively (Table 2). To further improve the device characteristics, the surface of the SiO₂ gate dielectric was treated with octadecyltrichlorosilane (ODTS) to form a self-assembled monolayer (SAM). With the modification of a ODTS-SAM layer, the hole mobilities of the PaADTDPP

Table 1. Summary of the Intrinsic Properties of the Polymers

polymer	T_d (°C)	T_m (°C)	E_g^{opta} (eV) (Film)	λ_{max} (nm)		HOMO (eV)	LUMO (eV)	E_g^{ecb}
				ODCB	film			
PaADTDPP	400		1.39	368, 736	368, 670, 736	-5.21	-3.61	1.60
PaADTT	434	285	2.13	318, 390, 479	314, 406, 513, 553	-5.41	-3.00	2.41

^a E_g^{opt} from the onset of UV spectra in thin film. ^b E_g^{ec} = electrochemical band gap (LUMO–HOMO).

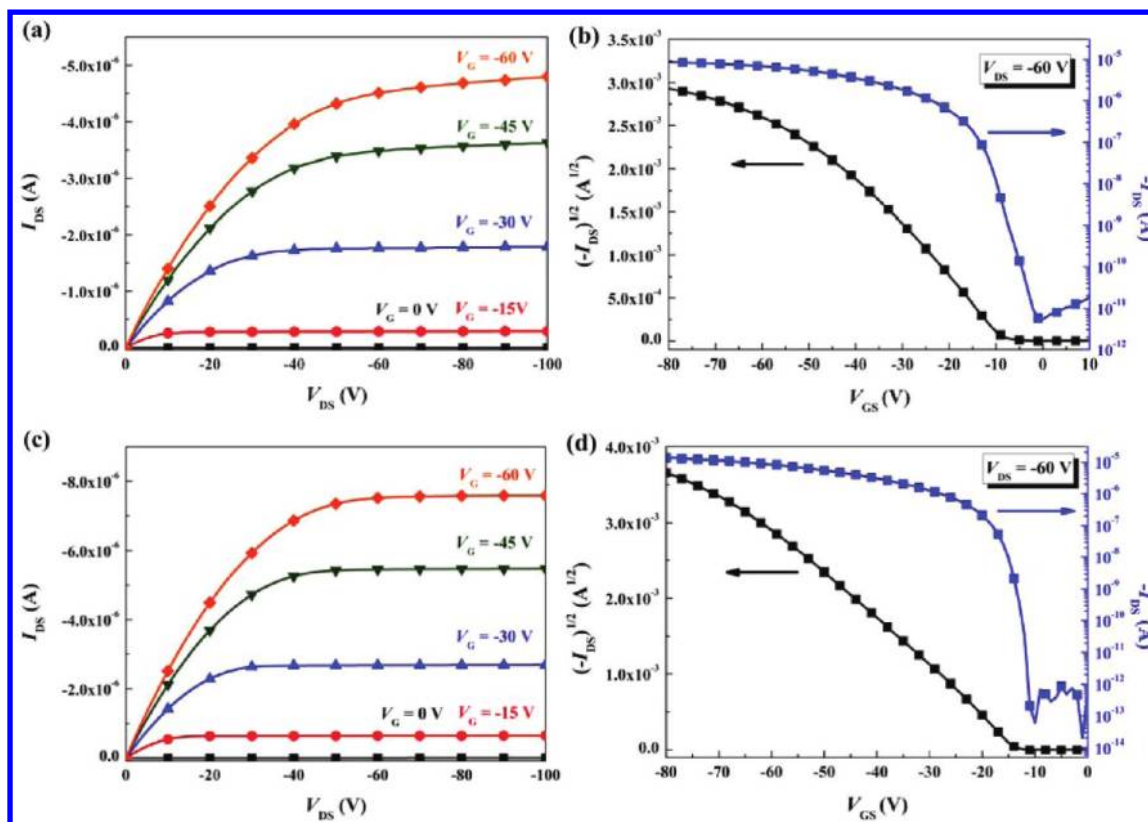


Figure 4. Typical output curves (a, c) and transfer plots (b, d) of the OFET devices based on PaADTDPP and PaADTT with ODTs-SAM layer, respectively.

Table 2. p-Type FET Characteristics of PaADTDPP and PaADTT Film

polymer	SAM layer	annealing ($^{\circ}\text{C}$)	mobility ($\text{cm}^2 \text{V}^{-1} \text{s}^{-1}$)	I (on/off)	V_t (V)
PaADTDPP	bare SiO_2	150	2.0×10^{-3}	3.1×10^3	18.8
PaADTDPP	bare SiO_2	250	9.4×10^{-3}	1.8×10^2	25.2
PaADTDPP	ODTS	150	2.2×10^{-2}	5.2×10^5	-2.9
PaADTDPP	ODTS	250	7.3×10^{-2}	1.6×10^6	-8.2
PaADTT	bare SiO_2	150	7.2×10^{-2}	5.1×10^6	-6.0
PaADTT	bare SiO_2	250	1.2×10^{-2}	1.9×10^6	-4.4
PaADTT	ODTS	150	7.9×10^{-2}	1.1×10^7	-13.0
PaADTT	ODTS	250	6.8×10^{-2}	1.5×10^8	-7.3

devices were significantly enhanced to $2.2 \times 10^{-2} \text{ cm}^2 \text{V}^{-1} \text{s}^{-1}$ and $7.3 \times 10^{-2} \text{ cm}^2 \text{V}^{-1} \text{s}^{-1}$ with the annealing temperature at 150 and 250 $^{\circ}\text{C}$, respectively. Accordingly, the on-off ratios were also dramatically improved to 5.2×10^5 and 1.6×10^6 . On the other hand, the mobilities of the PaADTT-based devices did not show distinct correlation with respect to the annealing temperatures. It was found that the PaADTT hole mobility is only slightly higher in the ODTs-modified device than the unmodified one due to the reason that order π - π stacking can also be formed on the bare SiO_2 due to the crystalline nature of PaADTT. PaADTT achieved the highest mobility of $7.9 \times 10^{-2} \text{ cm}^2 \text{V}^{-1} \text{s}^{-1}$ with an on-off ratio of 1.1×10^7 from the ODTs-modified device annealed at 150 $^{\circ}\text{C}$.

Photovoltaic Characteristics. Bulk heterojunction PSCs were fabricated on the basis of ITO/PEDOT:PSS/polymer:PC₇₁BM/Ca/Al configuration, and their performances were measured under 100 mW/cm² AM 1.5 illumination. The characterization data are summarized in Table 3, and the current density-voltage characteristics of these polymers are shown in Figure 5. The device based on

Table 3. PSCs Characteristics of PaADTDPP and PaADTT

polymer	blend ratio with PC ₇₁ BM	V_{oc} (V)	J_{sc} (mA/cm^2)	FF (%)	PCE (%)
PaADTDPP	1:2.5	0.66	9.49	58.4	3.66
PaADTDPP	1:2.5 ^a	0.66	10.66	60.2	4.24
PaADTT	1:1	0.80	3.46	63.8	1.77

^a1-Chloronaphthalene (1.5 vol %) in ODCB solution.

PaADTDPP:PC₇₁BM (1:2.5, w/w) blend exhibited a V_{oc} of 0.66 V, a J_{sc} of 9.49 mA/cm², and a FF of 58.4%, delivering an PCE of 3.66%. By judicious choice of the processing additives, nanoscale morphology of the active layer can be efficiently controlled and optimized.^{2b,15} Encouragingly, by adding 1.5 vol % 1-chloronaphthalene (CN) into ODCB as the processing additive, the PCE was improved to 4.24% as a result of the increased J_{sc} values. To gain more insight into the performance enhancement upon the introduction of CN additive, the morphology of the blend films was investigated by atomic force microscope (AFM) (Figure 6). Compared to the pristine film,

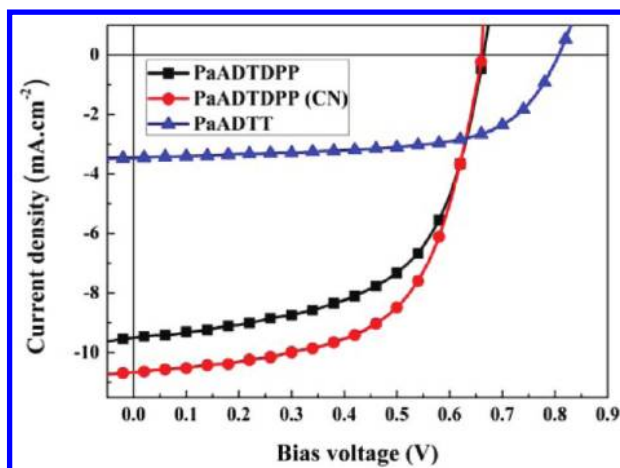


Figure 5. Current density–voltage characteristics of ITO/PE-DOT:PSS/polymer:PC₇₁BM/Ca/Al devices under illumination of AM 1.5 G at 100 mW/cm².

the additive-processed PaADTDPP:PC₇₁BM film showed small phase separation domains and more pronounced fiber-like nanostructures with greater surface roughness, suggesting its more favorable morphological property for efficient charge separation and transporting properties. On the other hand, the device using the PaADTT/PC₇₁BM blend (1:1, w/w) exhibited a V_{oc} of 0.80 V, a J_{sc} of 3.46 mA/cm², and a FF of 63.8%, leading to a PCE of 1.77%. Compared to PaADTDPP, the device based on PaADTT as the p-type material exhibited a

higher V_{oc} of 0.80 V due to the lower-lying HOMO level (−5.41 eV). However, the much lower J_{sc} resulting in the lower PCE might be due to the limited absorption range of PaADTT or energetically unfavorable charge transfer.

CONCLUSIONS

Structurally analogous to pentacene, linear-fused anthradithiophene derivatives have received a great deal of interest due to their high intrinsic mobilities and good chemical stability. However, compared to the devices based on IADT small molecules, solution-processable IADT-based conjugated polymers have not produced successful OPV and OFET device performance. Introducing sufficient aliphatic side chains to improve solubility and modulating molecular shape of the ADT system to optimize molecular packing provide effective solutions to overcome the deficiencies. In this regard, we have developed an elegant route to synthesize an angular-shaped and isomer-free anti-anthradithiophene moiety. The merit of the synthesis is that the construction of aADT framework and the introduction of aliphatic side chains are accomplished simultaneously by one-pot Suzuki-coupling benzannulation between a dialkyldiborylalkene and a dibromobiphenyl substrate. For the first time, the aADT unit was copolymerized with DPP and bithiophene monomers to prepare aADT-based conjugated polymers, PaADTDPP and PaADTT, respectively. The OPV device based on PaADTDPP/PC₇₁BM delivered a decent PCE of 4.24%, which is the highest value among the devices using the IADT-based polymers. Besides, PaADTT also achieved a high

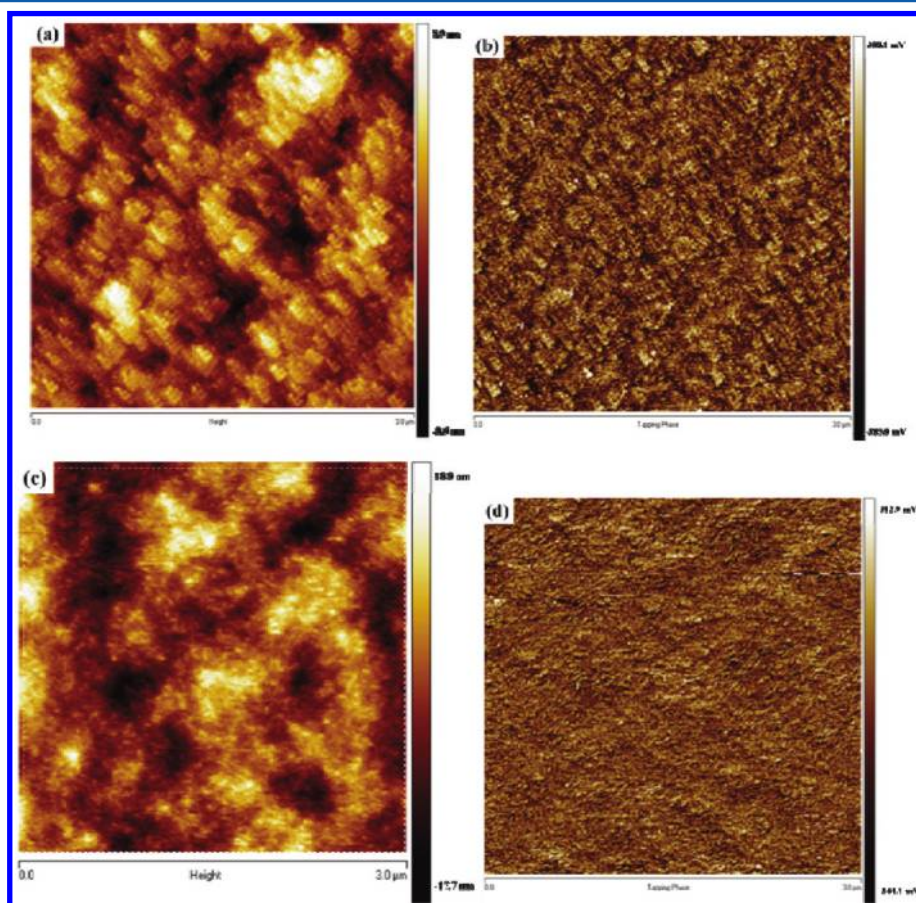


Figure 6. AFM height and phase images of the surface of PaADTDPP/PC₇₁BM blend (a, b) and PaADTDPP/PC₇₁BM (with 1.5 vol % CN) (c, d).

FET mobility of $7.9 \times 10^{-2} \text{ cm}^2 \text{ V}^{-1} \text{ s}^{-1}$ with an on–off ratio of 1.1×10^7 , which also outperforms the IADT-containing polymers reported in the literature.^{8b} Further optimization of the molecular properties of aADT-based polymers is highly achievable by modification of aliphatic substituents on aADT, or by copolymerization of the aADT monomer with various acceptors. Finally, this synthetic strategy will also be applicable for creating a range of new fascinating ladder-type conjugated structures. The follow-up research is currently underway in our laboratory.

EXPERIMENTAL SECTION

General Measurement and Characterization. All chemicals were purchased from Aldrich or Acros and used as received unless otherwise specified. ¹H and ¹³C NMR spectra were measured using a Varian 300 MHz instrument spectrometer. Differential scanning calorimeter (DSC) was measured on a TA Q200 Instrument, and thermogravimetric analysis (TGA) was recorded on a Perkin-Elmer Pyris under nitrogen atmosphere at a heating rate of 10 °C/min. Absorption spectra were collected on a HP8453 UV–vis spectrophotometer. The molecular weights of the polymers were measured by the GPC method on a Viscotek VE2001GPC, and polystyrene was used as the standard (THF as the eluent). The electrochemical cyclic voltammetry (CV) was conducted on a CH Instruments Model 611D. A carbon glass coated with a thin polymer film was used as the working electrode and Ag/Ag⁺ electrode as the reference electrode, while 0.1 M tetrabutylammonium hexafluorophosphate (Bu₄NPF₆) in acetonitrile was the electrolyte. CV curves were calibrated using ferrocene as the standard, whose oxidation potential is set at –4.8 eV with respect to the zero vacuum level. The HOMO energy levels were obtained from the equation $\text{HOMO} = -(E_{\text{ox}}^{\text{onset}} - E_{(\text{ferrocene})}^{\text{onset}} + 4.8) \text{ eV}$. The LUMO levels of polymer were obtained from the equation $\text{LUMO} = -(E_{\text{red}}^{\text{onset}} - E_{(\text{ferrocene})}^{\text{onset}} + 4.8) \text{ eV}$.

OFET Fabrication. An n-type heavily doped Si wafer with a SiO₂ layer of 300 nm and a capacitance of 11 nF/cm² was used as the gate electrode and dielectric layer. Thin films (40–60 nm in thickness) of polymers were deposited on octadecyltrichlorosilane (ODTS)-treated SiO₂/Si substrates by spin-coating their *o*-dichlorobenzene solutions (5 mg/mL). Then, the thin films were annealed at different temperatures (150 or 250 °C) for 30 min. Gold source and drain contacts (40 nm in thickness) were deposited by vacuum evaporation on the organic layer through a shadow mask, affording a bottom-gate, top-contact device configuration. Electrical measurements of OTFT devices were carried out at room temperature in air using a 4156C, Agilent Technologies. The field-effect mobility was calculated in the saturation regime by using the equation $I_{\text{ds}} = (\mu WC_i/2L)(V_g - V_t)^2$, where I_{ds} is the drain-source current, μ is the field-effect mobility, W is the channel width (1 mm), L is the channel length (100 μm), C_i is the capacitance per unit area of the gate dielectric layer, V_g is the gate voltage, and V_t is threshold voltage.

PSCs Fabrication. ITO/glass substrates were ultrasonically cleaned sequentially in detergent, water, acetone, and iso-propanol (IPA). The cleaned substrates were covered by a 30 nm thick layer of PEDOT:PSS (Clevios P provided by Stark) by spin coating. After annealing in a glovebox at 150 °C for 30 min, the samples were cooled to room temperature. Polymers were dissolved in *o*-dichlorobenzene (ODCB) or 1.5 vol % 1-chloronaphthalene (CN) ODCB solution, and then PC₇₁BM (purchased from Nano-C) was added. The solution was then heated at 80 °C and stirred overnight at the same temperature. Prior to deposition, the solution were filtered (1 μm filters). The solution of polymer:PC₇₁BM was then spin coated to form the active layer. The cathode made of calcium (350 nm thick) and aluminum (1000 nm thick) was sequentially evaporated through a shadow mask under high vacuum (<10^{–6} Torr). Each sample consists of four independent pixels defined by an active area of 0.04 cm². Finally, the devices were encapsulated and characterized in air. The devices were characterized under 100 mW/cm² AM 1.5 simulated light measurement (Yamashita Denso solar simulator). Current–voltage (J – V)

characteristics of PSC devices were obtained by a Keithley 2400 SMU. Solar illumination conforming the JIS Class AAA was provided by a SAN-EI 300W solar simulator equipped with an AM 1.5G filter. The light intensity was calibrated with a Hamamatsu S1336-SBK silicon photodiode.

Synthesis of 9-Octadecyne (2). To a solution of 1-decyne **1** (6.0 g, 43.4 mmol) in dry THF (60 mL) was added a 2.0 M solution of lithium diisopropylamide (LDA) in hexane (23.9 mL, 47.8 mmol) dropwise at 0 °C. After stirring at 0 °C for 1 h, 1-bromooctane (8.8 g, 45.6 mmol) was introduced by syringe to the solution. The mixture solution was warmed up to room temperature and refluxed at 60 °C for 12 h. The mixture solution was quenched with water and extracted with diethyl ether (100 mL × 3) and water (100 mL). The combined organic layer was dried over MgSO₄. After removal of the solvent under reduced pressure, the residue was distilled at 150 °C to remove impurities. The residue was purified by column chromatography on silica gel (hexane) to give a colorless liquid **2** (2.7 g, 25%). ¹H NMR (CDCl₃, 300 MHz, ppm): δ 0.88 (t, $J = 6.6 \text{ Hz}$, 6 H), 1.27–1.38 (m, 20 H), 1.45–1.49 (m, 4 H), 2.13 (t, $J = 6.9 \text{ Hz}$, 4 H). ¹³C NMR (CDCl₃, 75 MHz, ppm): δ 14.23, 18.91, 22.82, 29.04, 29.31, 29.34, 29.40, 32.02, 80.35. MS (EI, C₁₈H₃₄): calcd, 250.46; found, 250.

Synthesis of (Z)-1,2-Bis(4,4,5,5-tetramethyl-1,3,2-dioxaborolan-2-yl)-1,2-dioctylethene (3). The compound was synthesized by following the procedure in the literature.¹² 9-Octadecyne **2** (2.5 g, 9.98 mmol), bis(pinacolato)diboron (2.3 g, 9.07 mmol) and Pt(PPh₃)₄ (339 mg, 0.27 mmol) were dissolved in DMF (40 mL). The reaction mixture was stirred at 80 °C for 24 h and then extracted with diethyl ether (100 mL × 3) and water (150 mL). The collected organic layer was dried over MgSO₄. After removal of the solvent under reduced pressure, the residue was purified by column chromatography on silica gel (hexane/ethyl acetate, v/v, 25/1) to give a colorless liquid **3** (3.77 g, 75%). ¹H NMR (CDCl₃, 300 MHz, ppm): δ 0.85–0.89 (m, 6 H), 1.21–1.31 (m, 48 H), 2.16 (t, $J = 7.5 \text{ Hz}$, 4 H). ¹³C NMR (CDCl₃, 75 MHz, ppm): δ 14.24, 22.83, 25.03, 29.36, 29.62, 29.88, 30.16, 30.97, 32.05, 83.36. MS (EI, C₃₀H₅₈B₂O₄): calcd, 504.4; found, 504. Elemental analysis (%) calcd for C₃₀H₅₈B₂O₄: C, 71.44; H, 11.59. Found: C, 71.23; H, 11.34.

Synthesis of (3-Bromothiophen-2-yl)zinc(II)bromide (5). To a solution of 2,3-dibromothiophene **4** (6.25 g, 25.8 mmol) in dry THF (20 mL) was added a 2.5 M solution of *n*-BuLi in hexane (11.1 mL, 27.7 mmol) dropwise at –78 °C. After stirring at –78 °C for 1 h, the mixture solution was warmed up to room temperature. The mixture solution was added to a solution of zinc(II)bromide (5.82 g, 25.8 mmol) in dry THF (15 mL) at –78 °C, and then the mixture solution was stirred at 0 °C for 1 h.

Synthesis of 2,2'-(2,5-Dibromo-1,4-phenylene)bis(3-bromothiophene) (7). To a solution of 1,4-dibromo-2,5-diiodobenzene **6** (4.50 g, 9.2 mmol) and Pd(PPh₃)₄ (0.27 g, 0.23 mmol) in dry THF (30 mL) was added a solution of (3-bromothiophen-2-yl)zinc(II)-bromide **5** (25.8 mmol) at room temperature. The mixture solution was refluxed for 3 h. After removal of the solvent under reduced pressure, the residue was extracted with ethyl acetate (250 mL × 3) and water (150 mL). The collected organic layer was dried over MgSO₄. After removal of the solvent under reduced pressure, the residue was purified by column chromatography on silica gel (hexane) to give a white solid product **7** (1.54 g, 30%). ¹H NMR (CDCl₃, 300 MHz, ppm): δ 7.09 (d, $J = 5.4 \text{ Hz}$, 2 H), 7.42 (d, $J = 5.4 \text{ Hz}$, 2 H), 7.71 (s, 2 H). ¹³C NMR (CDCl₃, 75 MHz, ppm): δ 111.79, 123.53, 126.97, 130.51, 135.19, 136.13, 136.64.

Synthesis of aADT. The compound was synthesized by following the procedure in the literature.¹⁴ 2,2'-(2,5-Dibromo-1,4-phenylene)-bis(3-bromothiophene) **7** (500 mg, 0.90 mmol), (Z)-1,2-bis(4,4,5,5-tetramethyl-1,3,2-dioxaborolan-2-yl)-1,2-dioctylethene **3** (1.04 g, 2.06 mmol), K₂CO₃ (1.49 g, 10.78 mmol), and Pd(PPh₃)₄ (104 mg, 0.09 mmol) were dissolved in deoxygenated THF/H₂O (40 mL/2.1 mL). The mixture was then degassed by bubbling nitrogen for 5 min at room temperature. The reaction mixture was refluxed at 65 °C for 48 h and then extracted with diethyl ether (100 mL × 3) and water (150 mL). The collected organic layer was dried over MgSO₄. After removal of the solvent under reduced pressure, the residue was

purified by column chromatography on silica gel (hexane) to give a pale yellow solid aADT (392 mg, 59%). ¹H NMR (CDCl₃, 300 MHz, ppm): δ 0.88 (br, 12 H), 1.30–1.49 (m, 40 H), 1.61–1.79 (m, 8 H), 3.08 (t, J = 8.1 Hz, 4 H), 3.25 (t, J = 7.8 Hz, 4 H), 7.50 (d, J = 5.4 Hz, 2 H), 7.55 (d, J = 5.4 Hz, 2 H), 8.80 (s, 2H). ¹³C NMR (CDCl₃, 75 MHz, ppm): δ 14.28, 14.31, 22.85, 22.86, 28.69, 29.50, 29.55, 29.69, 29.85, 30.43, 30.48, 31.13, 31.28, 31.47, 32.08, 32.10, 119.82, 124.10, 124.60, 127.01, 128.75, 131.81, 133.18, 136.48, 137.59. MS (FAB, C₅₀H₇₄S₂): calcd, 739.25; found, 739. Elemental analysis (%) calcd for C₅₀H₇₄S₂: C, 81.24; H, 10.09. Found: C, 81.30; H, 10.27.

Synthesis of Sn-aADT. To a solution of aADT (392 mg, 0.53 mmol) in dry THF (20 mL) was added a 1.6 M solution of *t*-BuLi in hexane (0.83 mL, 1.33 mmol) dropwise at –78 °C. (Precaution: *tert*-butyllithium is a pyrophoric substance that spontaneously catches fire on exposure to air and thus should be handled with a glass syringe and inert gas flushing equipment.) After stirring at –78 °C for 1 h, a 1.0 M solution of chlorotrimethylstannane in THF (2.7 mL, 2.7 mmol) was introduced by syringe to the solution. The mixture solution was warmed up to room temperature and stirred for 12 h. The mixture solution was quenched with water and extracted with diethyl ether (50 mL × 3) and water (50 mL). After removal of the solvent under reduced pressure, compound Sn-aADT was obtained as pale yellow solid (558 mg, 99%). ¹H NMR (CDCl₃, 300 MHz, ppm): δ 0.48 (s, 18 H), 0.85–0.90 (m, 12 H), 1.28–1.35 (m, 40 H), 1.61–1.76 (m, 8 H), 3.10 (t, J = 8.1 Hz, 4 H), 3.25 (t, J = 7.8 Hz, 4 H), 7.57 (s, 2 H), 8.81 (s, 2 H). MS (FAB, C₅₆H₉₀S₂Sn₂): calcd, 1064.86; found, 1065.

Synthesis of PaADTDP. To a 50 mL round-bottom flask was introduced Sn-aADT (230.0 mg, 0.216 mmol), **8** (147.4 mg, 0.216 mmol), tris(dibenzylideneacetone) dipalladium (9.9 mg, 0.011 mmol), tri(2-methylphenyl)phosphine (26.3 mg, 0.086 mmol), and deoxygenated chlorobenzene (7 mL). The mixture was then degassed by bubbling nitrogen for 10 min at room temperature. The round-bottom flask was placed into the microwave reactor and reacted at 180 °C for 50 min under 270 W. Then, tributyl(thiophen-2-yl)stannane (40.3 mg, 0.108 mmol) was added to the mixture solution and reacted for 10 min under 270 W. Finally, 2-bromothiophene (19.4 mg, 0.119 mmol) was added to the mixture solution and reacted for 10 min under 270 W. The solution was added into methanol dropwise. The precipitate was collected by filtration and washed by Soxhlet extraction with acetone (24 h), hexane (24 h), and THF (24 h) sequentially. The product was redissolved in hot *o*-dichlorobenzene (100 mL). The Pd–thiol gel (Silicycle Inc.) was added to the above *o*-dichlorobenzene solution to remove the residual Pd catalyst at 130 °C for 6 h. After filtration of the solution, the polymer solution was added into methanol to reprecipitate. The purified polymer was collected by filtration and dried under vacuum for 1 day to give a purplish black solid (71 mg, yield 26%).

Synthesis of PaADTT. To a 50 mL round-bottom flask was introduced Sn-aADT (117.6 mg, 0.110 mmol), **9** (79.1 mg, 0.110 mmol), tris(dibenzylideneacetone) dipalladium (5.0 mg, 0.0055 mmol), tri(2-methylphenyl)phosphine (13.4 mg, 0.044 mmol), and deoxygenated chlorobenzene (3.6 mL). The mixture was then degassed by bubbling nitrogen for 10 min at room temperature. The round-bottom flask was placed into the microwave reactor and reacted at 180 °C for 50 min under 270 W. Then, tributyl(thiophen-2-yl)stannane (20.5 mg, 0.055 mmol) was added to the mixture solution and reacted for 10 min under 270 W. Finally, 2-bromothiophene (9.9 mg, 0.061 mmol) was added to the mixture solution and reacted for 10 min under 270 W. The solution was added into methanol dropwise. The precipitate was collected by filtration and washed by Soxhlet extraction with acetone (24 h) and hexane (24 h) sequentially. The product was redissolved in hot toluene (100 mL). The Pd–thiol gel (Silicycle Inc.) was added to the above toluene solution to remove the residual Pd catalyst at 80 °C for 12 h. After filtration of solution and removal of the solvent under reduced pressure, the polymer solution was added into methanol to reprecipitate. The purified polymer was collected by filtration and dried under vacuum for 1 day to give a red black solid (90 mg, yield 63%). ¹H NMR (CDCl₃, 300 MHz, ppm): δ 0.83–0.91 (m, 18 H), 1.22–1.48 (m, 84 H), 1.79 (br, 12 H), 2.93

(br, 4 H), 3.09 (br, 4 H), 3.26 (br, 4 H), 7.14 (br, 2 H), 7.54 (br, 2 H), 8.75 (br, 2 H).

■ ASSOCIATED CONTENT

Supporting Information

TGA measurements of polymers and ¹H NMR spectra of the new compounds. This material is available free of charge via the Internet at <http://pubs.acs.org>.

■ AUTHOR INFORMATION

Corresponding Author

*E-mail: yjcheng@mail.nctu.edu.tw; cshsu@mail.nctu.edu.tw.

Notes

The authors declare no competing financial interest.

■ ACKNOWLEDGMENTS

This work is supported by the National Science Council and “ATP” of the National Chiao Tung University and Ministry of Education, Taiwan.

■ REFERENCES

- (1) (a) Arias, A. C.; MacKenzie, J. D.; McCulloch, I.; Rivnay, J.; Salleo, A. *Chem. Rev.* **2010**, *110*, 3. (b) Yu, G.; Gao, J.; Hummelen, J. C.; Wudl, F.; Heeger, A. J. *Science* **1995**, *270*, 1789. (c) Günes, S.; Neugebauer, H.; Sariciftci, N. S. *Chem. Rev.* **2007**, *107*, 1324. (d) Thompson, B. C.; Fréchet, J. M. J. *Angew. Chem., Int. Ed.* **2008**, *47*, 58. (e) Cheng, Y.-J.; Yang, S.-H.; Hsu, C.-S. *Chem. Rev.* **2009**, *109*, 5868. (f) Chen, J.; Cao, Y. *Acc. Chem. Res.* **2009**, *42*, 1709. (g) Li, Y.; Zou, Y. *Adv. Mater.* **2008**, *20*, 2952.
- (2) (a) He, F.; Wang, W.; Chen, W.; Xu, T.; Darling, S. B.; Strzalka, J.; Liu, Y.; Yu, L. *J. Am. Chem. Soc.* **2011**, *133*, 3284. (b) Chang, C.-Y.; Cheng, Y.-J.; Hung, S.-H.; Wu, J.-S.; Kao, W.-S.; Lee, C.-H.; Hsu, C.-S. *Adv. Mater.* **2012**, *24*, 549. (c) Zhang, Y.; Zou, J.; Yip, H.-L.; Chen, K.-S.; Zeigler, D. F.; Sun, Y.; Jen, A. K.-Y. *Chem. Mater.* **2011**, *23*, 2289. (d) Cheng, Y.-J.; Wu, J.-S.; Shih, P.-I.; Chang, C.-Y.; Jwo, P.-C.; Kao, W.-S.; Hsu, C.-S. *Chem. Mater.* **2011**, *23*, 2361. (e) Wu, J.-S.; Cheng, Y.-J.; Dubosc, M.; Hsieh, C.-H.; Chang, C.-Y.; Hsu, C.-S. *Chem. Commun.* **2010**, *46*, 3259. (f) Wu, J.-S.; Cheng, Y.-J.; Lin, T.-Y.; Chang, C.-Y.; Shih, P.-I.; Hsu, C.-S. *Adv. Funct. Mater.* **2012**, *22*, 1711. (g) Wang, J.-Y.; Hau, S. K.; Yip, H.-L.; Davies, J. A.; Chen, K.-S.; Zhang, Y.; Sun, Y.; Jen, A. K.-Y. *Chem. Mater.* **2011**, *23*, 765. (h) Ashraf, R. S.; Chen, Z.; Leem, D. S.; Bronstein, H.; Zhang, W.; Schroeder, B.; Geerts, Y.; Smith, J.; Watkins, S.; Anthopoulos, T. D.; Sirringhaus, H.; de Mello, J. C.; Heeney, M.; McCulloch, I. *Chem. Mater.* **2011**, *23*, 768. (i) Chen, C.-H.; Cheng, Y.-J.; Dubosc, M.; Hsieh, C.-H.; Chu, C.-C.; Hsu, C.-S. *Chem. Asian J.* **2010**, *5*, 2480. (j) Zhang, M.; Guo, X.; Wang, X.; Wang, H.; Li, Y. *Chem. Mater.* **2011**, *23*, 4264. (k) Cheng, Y.-J.; Chen, C.-H.; Lin, Y.-S.; Chang, C.-Y.; Hsu, C.-S. *Chem. Mater.* **2011**, *23*, 5068. (l) Chen, C.-H.; Cheng, Y.-J.; Chang, C.-Y.; Hsu, C.-S. *Macromolecules* **2011**, *44*, 8415. (m) Cheng, Y.-J.; Ho, Y.-J.; Chen, C.-H.; Kao, W.-S.; Wu, C.-E.; Hsu, S.-L.; Hsu, C.-S. *Macromolecules* **2012**, *45*, 2690. (n) Cheng, Y.-J.; Cheng, S.-W.; Chang, C.-Y.; Kao, W.-S.; Liao, M.-H.; Hsu, C.-S. *Chem. Commun.* **2012**, *48*, 3203. (o) Forster, M.; Annan, K. O.; Scherf, U. *Macromolecules* **1999**, *32*, 3159. (p) Scherf, U. *J. Mater. Chem.* **1999**, *9*, 1853. (q) Chmil, K.; Scherf, U. *Acta Polym.* **1997**, *48*, 208. (r) Chmil, K.; Scherf, U. *Makromol. Chem., Rapid Commun.* **1993**, *14*, 217. (s) Facchetti, A. *Chem. Mater.* **2011**, *23*, 733. (t) Guo, X.; Ortiz, R. P.; Zheng, Y.; Hu, Y.; Noh, Y.-Y.; Baeg, K.-J.; Facchetti, A.; Marks, T. J. *J. Am. Chem. Soc.* **2011**, *133*, 1405. (u) Loser, S.; Bruns, C. J.; Miyauchi, H.; Ortiz, R. P.; Facchetti, A.; Stupp, S. I.; Marks, T. J. *J. Am. Chem. Soc.* **2011**, *133*, 8142. (3) (a) Takimiya, K.; Shinamura, S.; Osaka, I.; Miyazaki, E. *Adv. Mater.* **2011**, *23*, 4347. (b) Huo, L.; Hou, J. *Polym. Chem.* **2011**, *2*, 2453. (c) Anthony, J. E. *Chem. Rev.* **2006**, *106*, 5028.

- (4) (a) Shinamura, S.; Osaka, I.; Miyazaki, E.; Nakao, A.; Yamagishi, M.; Takeya, J.; Takimiya, K. *J. Am. Chem. Soc.* **2011**, *133*, 5024. (b) Osaka, I.; Abe, T.; Shinamura, S.; Miyazaki, E.; Takimiya, K. *J. Am. Chem. Soc.* **2010**, *132*, 5000. (c) Niimi, K.; Shinamura, S.; Osaka, I.; Miyazaki, E.; Takimiya, K. *J. Am. Chem. Soc.* **2011**, *133*, 8732. (d) Dickey, K. C.; Anthony, J. E.; Loo, Y.-L. *Adv. Mater.* **2006**, *18*, 1721. (e) Goetz, K. P.; Li, Z.; Ward, J. W.; Bougher, C.; Rivnay, J.; Smith, J.; Conrad, B. R.; Parkin, S. R.; Anthopoulos, T. D.; Salleo, A.; Anthony, J. E.; Jurchescu, O. D. *Adv. Mater.* **2011**, *23*, 3698.
- (5) (a) Zhou, H.; Yang, L.; Stuart, A. C.; Price, S. C.; Liu, S.; You, W. *Angew. Chem., Int. Ed.* **2011**, *50*, 2995. (b) Huo, L.; Zhang, S.; Guo, X.; Xu, F.; Li, Y.; Hou, J. *Angew. Chem., Int. Ed.* **2011**, *50*, 9697. (c) Boudreault, P.-L. T.; Najari, A.; Leclerc, M. *Chem. Mater.* **2011**, *23*, 456. (d) Zou, Y.; Najari, A.; Berrouard, P.; Beaupré, S.; Aïch, B. R.; Tao, Y.; Leclerc, M. *J. Am. Chem. Soc.* **2010**, *132*, 5330. (e) Piliago, C.; Holcombe, T. W.; Douglas, J. D.; Woo, C. H.; Beaujuge, P. M.; Fréchet, J. M. J. *J. Am. Chem. Soc.* **2010**, *132*, 7595. (f) Pan, H.; Li, Y.; Wu, Y.; Liu, P.; Ong, B. S.; Zhu, S.; Xu, G. *J. Am. Chem. Soc.* **2007**, *129*, 4112.
- (6) (a) Wolak, M. A.; Jang, B. B.; Palilis, L. C.; Kafafi, Z. H. *J. Phys. Chem. B* **2004**, *108*, 5492. (b) Li, Y.; Wu, Y.; Liu, P.; Prostran, Z.; Gardner, S.; Ong, B. S. *Chem. Mater.* **2007**, *19*, 418. (c) Allen, C. F.; Bell, A. *J. Am. Chem. Soc.* **1942**, *64*, 1253. (d) Maliakal, A.; Raghavachari, K.; Katz, H.; Chandross, E.; Siegrist, T. *Chem. Mater.* **2004**, *16*, 4980. (e) Yamada, M.; Ikemote, I.; Kuroda, H. *Bull. Chem. Soc. Jpn.* **1988**, *61*, 1057. (f) Kaur, I.; Jia, W.; Kopreski, R. P.; Selvarasah, S.; Dokmeci, M. R.; Pramanik, C.; McGruer, N. E.; Miller, G. P. *J. Am. Chem. Soc.* **2008**, *130*, 16274.
- (7) (a) Wang, J.; Liu, K.; Liu, Y.-Y.; Song, C.-L.; Shi, Z.-F.; Peng, J.-B.; Zhang, H.-L.; Cao, X.-P. *Org. Lett.* **2009**, *11*, 2563. (b) Laquindanum, J. G.; Katz, H. E.; Lovinger, A. J. *J. Am. Chem. Soc.* **1998**, *120*, 664. (c) Payne, M. M.; Parkin, S. R.; Anthony, J. E.; Kuo, C.-C.; Jackson, T. N. *J. Am. Chem. Soc.* **2005**, *127*, 4986. (d) Lee, W. H.; Kwak, D.; Anthony, J. E.; Lee, H. S.; Choi, H. H.; Kim, D. H.; Lee, S. G.; Cho, K. *Adv. Funct. Mater.* **2012**, *22*, 267. (e) Jurchescu, O. D.; Subramanian, S.; Kline, R. J.; Hudson, S. D.; Anthony, J. E.; Jackson, T. N.; Gundlach, D. J. *Chem. Mater.* **2008**, *20*, 6733.
- (8) (a) Okamoto, T.; Jiang, Y.; Qu, F.; Mayer, A. C.; Parmer, J. E.; McGehee, M. D.; Bao, Z. *Macromolecules* **2008**, *41*, 6977. (b) Jiang, Y.; Okamoto, T.; Becerril, H. A.; Hong, S.; Tang, M. L.; Mayer, A. C.; Parmer, J. E.; McGehee, M. D.; Bao, Z. *Macromolecules* **2010**, *43*, 6361.
- (9) (a) Tylleman, B.; Vande Velde, C. M. L.; Balandier, J.-Y.; Stas, S.; Sergeev, S.; Geerts, Y. H. *Org. Lett.* **2011**, *13*, 5208. (b) Lloyd, M. T.; Mayer, A. C.; Subramian, S.; Mourey, D. A.; Herman, D. J.; Bapat, A. V.; Anthony, J. E.; Malliaras, G. G. *J. Am. Chem. Soc.* **2007**, *129*, 9144. (c) Chen, M. C.; Kim, C.; Chen, S.-Y.; Chiang, Y.-J.; Chung, M. C.; Facchetti, A.; Marks, T. J. *J. Mater. Chem.* **2008**, *18*, 1029.
- (10) Osaka, I.; Abe, T.; Shinamura, S.; Takimiya, K. *J. Am. Chem. Soc.* **2011**, *133*, 6852.
- (11) (a) Pietrangelo, A.; Patrick, B. O.; MacLachlan, M. J.; Wolf, M. O. *J. Org. Chem.* **2009**, *74*, 4918. (b) Pietrangelo, A.; MacLachlan, M. J.; Wolf, M. O.; Patrick, B. O. *Org. Lett.* **2007**, *9*, 3571.
- (12) Ishiyama, T.; Matsuda, N.; Miyaura, N.; Suzuki, A. *J. Am. Chem. Soc.* **1993**, *115*, 11018.
- (13) Hart, H.; Harada, K.; Du, C. J. *F. J. Org. Chem.* **1985**, *50*, 3104.
- (14) Shimizu, M.; Nagao, I.; Tomioka, Y.; Hiyama, T. *Angew. Chem., Int. Ed.* **2008**, *47*, 8096.
- (15) (a) Peet, J.; Kim, J. Y.; Coates, N. E.; Ma, W. L.; Moses, D.; Heeger, A. J.; Bazan, G. C. *Nat. Mater.* **2007**, *6*, 497. (b) Chen, L. M.; Hong, Z.; Li, G.; Yang, Y. *Adv. Mater.* **2009**, *21*, 1434. (c) Hoven, C. V.; Dang, X. D.; Coffin, R. C.; Peet, J.; Nguyen, T. Q.; Bazan, G. C. *Adv. Mater.* **2010**, *22*, E63.